Gap solitons and Bloch waves of interacting bosons in one-dimensional optical lattices: From the weak- to the strong-interaction limits

T.F. Xu, X.M. Guo, X.L. Jing, W.C. Wu, and C.S. Liu

Phys. Rev. A **83**, 043610 — Published 14 April 2011

DOI: 10.1103/PhysRevA.83.043610

Gap solitons and Bloch waves of interacting bosons in one-dimensional optical lattices: From the weak to the strong interaction limits

T. F. Xu[1], X. M. Guo[1], X. L. Jing[1], W. C. Wu[2], and C. S. Liu[1,2]
[1] *College of Science, Yanshan University, Qinhuangdao 066004, China*
[2] *Department of Physics, National Taiwan Normal University, Taipei 11677, Taiwan*
(Dated: March 4, 2011)

We study the gap solitons and nonlinear Bloch waves of interacting bosons in one-dimensional optical lattices, taking into account the interaction from the weak to the strong limits. It is shown that composition relation between the gap solitons and nonlinear Bloch waves exists for the whole span of the interaction strength. The linear stability analysis indicates that the gap solitons are stable when their energies are near the bottom of the linear Bloch band gap. By increasing the interaction strength, the stable gap solitons can turn into unstable. It is argued that the stable gap solitons can easily be formed in a weakly interacting system with energies near the bottoms of the lower-level linear Bloch band gaps.

PACS numbers: 42.65.Tg, 03.75.Lm, 42.65.Jx

I. INTRODUCTION

Recent development of trapping and cooling techniques has enabled experimental realizations of Bose-Einstein condensation (BEC) of bosonic atoms and molecules in optical lattices [1]. When the temperature is low and density is high, strong interaction between particles can result in significant nonlinearity in these systems. Associated with the periodicity and nonlinearity, there exist two important waves in these systems, namely Bloch waves and gap solitons. Bloch waves, which exist in both linear and nonlinear periodic systems, are extensive and spread over the whole space [2]. On the contrary, gap solitons, which are spatially localized atomic wave packets, exist only in a nonlinear periodic system [3]. In particular, a class of solitons called the fundamental gap solitons (FGSs), have the major peak well localized within a unit cell [4]. The solitons with two peaks of opposite signs within a unit cell are called the subfundamental solitons [5]. The relationship between the nonlinear Bloch waves (NLBWs) and the gap solitons is a topic of considerable interest.

Both FGSs and NLBWs can be simultaneously obtained by solving numerically the nonlinear Schrödinger equation of the system. For the weakly interacting one-dimensional (1D) periodic Bose system, it has been shown that NLBW can be regarded as the superposition of FGSs in an infinitely-long chain [6, 7]. This, so-called the "composition relation", leads to the prediction that there are n families of FGSs in the nth band gap of the corresponding linear periodic system. It also implies that a class of solutions similar to the Bloch waves can be built from it. It is interesting to see whether the composition relation remains correct in a strongly interacting system? To what extent the FGSs and NLBWs change when the interaction changes?

As is well known, mean-field theory typically does not work well for a 1D system, except in the very weakly interacting regime. The enhanced quantum fluctuation is significant in 1D quantum systems [8–11] which exhibit fascinating phenomena significantly different from their three-dimensional counterparts. On the other hand, for a single-component Bose gas in a harmonic trap, it has been shown that with the increase of the repulsive interaction, the density profile evolves continuously from a Gaussian-like distribution of bosons to a shell-structured distribution of fermions, called the Tonks-Girardeau (TG) gas [12, 13]. Thus when the interaction is strong, non-perturbative methods such as the Bose-Fermi mapping [14] or the Bethe ansatz [15, 16] need to be used to characterize the features of the system properly. Recently 1D harmonic trapped spinless Bose systems with a repulsive δ-function interaction have been solved in the limit of $N \to \infty$ [10, 17, 18]. Moreover, considering the two-component Bose gas with spin-independent interactions in the absence of the external potential, the ground-state energy density function has been extracted from the Bethe-ansatz solution. With the local-density approximation, a modified coupled nonlinear Schrödinger equations for the ground state has been obtained [19]. Using this kind of nonlinear Schrödinger equation, one is able to study the interplay between the periodicity and the nonlinearity in a 1D Bose system, especially for the interaction from the weak to the strong limits.

In this paper, we attempt to study the NLBWs and FGSs of an interacting Bose system in a 1D optical lattices. In particular, we are interested in how the NLBWs and FGSs of the system change when the interaction is changed from the weak to the strong limits, and whether the composition relation remains correct upon the change of the interaction. It will be shown that the composition relation remains valid in all interaction regimes. However, linear stability analysis indicates that stability of the soliton waves will change with the change of the nonlinearity.

The paper is organized as follows. In Sec. II, we introduce the model equation for a 1D interacting Bose system in optical lattices to which the interaction can be changed from the weak to the strong limits continuously. Sec. III

is devoted to compute the ground-state wave functions and energies of the system for the interaction from the weak to the strong limits. It is aimed to give a direct insight of the interaction dependent ground-state properties. By giving as much as possible evidence numerically in Sec. IV, we show that the composition relation exists between the NLBWs and FGSs in all interaction regimes. A generalized composition relation between the high-order solitons and multiple periodic waves is also shown. In Sec. V, the stabilities of various soliton waves are investigated upon the changes of the interaction and the strength of the periodic potential. Sec. VI is a brief summary.

II. MODEL EQUATION

We consider a 1D periodic Bose system described by the following time-dependent nonlinear Schrödinger equation

$$i\hbar\frac{\partial\Psi(x,t)}{\partial t}=\left[-\frac{\hbar^2}{2m}\frac{d^2}{dx^2}+V(x)+F\left(\rho\right)\right]\Psi(x,t), \quad (1)$$

where $V(x)=v\cos(\frac{2\pi}{\Lambda}x)$ is the periodic potential with Λ the lattice constant and v the strength and $F\left(\rho\right)$ is responsible for the interaction energy. The particle number is determined via $N=\int_{-\infty}^{\infty}\rho dx$ with $\rho=|\Psi|^2$. To go beyond the weak interaction limit, we use the following nonlinear form for $F\left(\rho\right)$ [19],

$$F\left(\rho\right)=\frac{\hbar^2\rho^2}{2m}\left[3e\left(\gamma\right)-\gamma\partial_\gamma e\left(\gamma\right)\right], \quad (2)$$

where

$$e\left(\gamma\right)=\frac{\gamma\left(1+p\gamma\pi^2/3\right)}{1+q\gamma+p\gamma^2}. \quad (3)$$

The results of Eqs. (2) and (3) were recently obtained by Hao and Chen based on Bethe Ansatz [19]. They can be equivalently obtained by solving exactly the equation for $e(\gamma)$ [see, for example, Eq. (6) in Ref. [10]], as done, for instance in Ref. [10]. Here $\gamma\equiv c/\rho$ with $c\equiv mg/\hbar^2$ (g is the scattering length) and $p=-5.0489470$ and $q=-20.8604983$ are the fitting parameters [19]. In the weakly ($\gamma\ll 1$) and strongly ($\gamma\gg 1$) interacting limits, one has the asymptotic forms

$$F\left(\rho\right)=\begin{cases}\dfrac{mg}{\hbar^2}\rho\sim|\Psi|^2, & \gamma\ll 1\\ \dfrac{\pi^2\hbar^2}{2m}\rho^2\sim|\Psi|^4, & \gamma\gg 1.\end{cases} \quad (4)$$

For convenience, dimensionless scaling will be made for the length and the energy [6, 7]. Position x is to be scaled in the unit of $\Lambda/(2\pi)$; Periodic potential $V(x)$, interaction energy $F(\rho)$, and the chemical potential μ are scaled in the unit of $8E_r$ with $E_r=\hbar^2\pi^2/2m\Lambda^2$ being the recoil energy and m the atom mass. Wave functions of both Bloch waves and gap solitons in optical lattices all have the form $\Psi(x,t)=\Phi(x)\exp(-i\mu t)$. Substituting it into the time-dependent nonlinear Schrödinger equation (1), one obtains the following dimensionless time-independent nonlinear Schrödinger equation

$$\left[-\frac{1}{2}\frac{d^2}{dx^2}+v\cos(x)+F\left(\rho\right)\right]\Phi(x)=\mu\Phi(x). \quad (5)$$

Eq. (5) is the starting point of the calculations throughout this paper.

III. GROUND-STATE PROPERTIES

By solving Eq. (5) numerically, one is able to obtain the ground-state density profile $\rho(x)$ and the corresponding chemical potential μ. It is remarked that to solve Eq. (5), we first differentiate it using the finite-element method along with the periodic boundary condition [20], and then evaluate several hundreds of steps in imaginary time until the lowest chemical potential μ is reached. In the calculation, the system is taken to be 16 lattice constant long (x ranges from -16π to 16π), the strength of periodic potential $v=1.5$, and the particle number $N=48$ (average 3 particles per unit cell). Figure 1(a) shows the density profile $\rho(x)$ within a unit cell. In view of Fig. 1(a), similar to the case of the Bose gas in a single harmonic trap, $\rho(x)$ evolves from the Bose distribution to the Fermi-like one when the interaction constant c is increased. In the weakly interacting regime ($c=0.2$), the density profile displays a Gaussian-like Bose distribution. When c is increased (see, for example, the case of $c=2$), density profile decreases at the center while increases at the two sides. In the extremely strong interaction regime ($c=500$), due to the strong enhancement of particle tunnelling rate across neighboring wells, density profile at the boundary increases significantly. In such limit, so-called the TG gas, the system will behave similar to the noninteracting fermions [21].

In order to compare the results obtained by the imaginary-time method, we also calculate the (exact) density profiles for the TG gas using the Bose-Fermi mapping method. In this case, Eq. (5) is first solved by the finite-element method by setting $F(\rho)=0$. The density profile is then calculated via $\rho_{\rm TG}(x)=\sum_{n=1}^{48}|\Phi_n(x)|^2$ with $\Phi_n(x)$ denoting the n-th energy eigenstate of the Hamiltonian. It turns out that the curve of $\rho_{\rm TG}(x)$ agrees well with the $\rho(x)$ obtained by the imaginary-time method for the large $c=500$ case [see Fig. 1(a)]. We notice that in addition to the central peak, $\rho_{\rm TG}(x)$ exhibits two humps at two sides near the center. Since the bottom of a single well behaves as an harmonic potential, the density $\rho_{\rm TG}(x)$ obtained by us is very similar to the Tonks density for three bosons in an harmonic potential. Three is exactly the number of particles put on average in a single well. It has been shown that by increasing the number of particles, the number of humps increases correspondingly while their amplitude decreases [22].

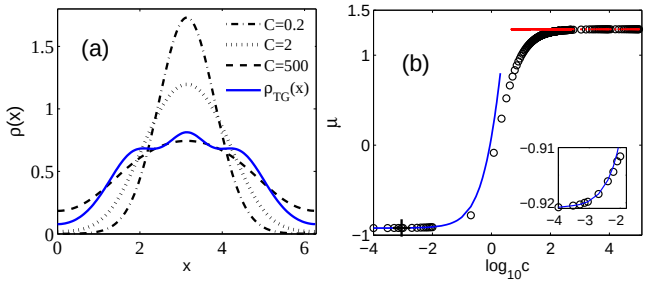

FIG. 1. (Color online) Panel (a): The interaction constant c-dependent ground-state density distribution $\rho(x)$ within one unit cell. Dimensionless x ranges from 0 to 2π for one unit length. The large $c = 500$ case is seen to behave like the non-interacting fermions (blue line, see text). Panel (b): The c-dependent ground-state chemical potentials calculated in the weak limit ($F(\rho) \sim |\Phi|^2$, blue line), in the strong limit ($F(\rho) \sim |\Phi|^4$, red line), and for a full $F(\rho)$ (circle line) respectively. The inset shows an enlarged view of the curves at small c's. The mark "+", corresponding to $c = 0.0009$, is what used in Ref. [6] to discuss the nonlinear bands.

It is well known that the dilute Bose-condensed gas can be described by the Gross-Pitaevskii (GP) mean-field (MF) theory [23]. In fact, MF approximation is only appropriate for a long-wavelength theory. For short-range repulsive interactions, MF theory fails in dimension $d < 2$ to which the nonlinear term $F(\rho) \sim |\Phi|^2$ in the GP MF theory should be replaced by $F(\rho) \sim |\Phi|^4$ from the renormalization group analysis [24]. One may ask to what extent the current system under studies will approach the above two (weak and strong) limits upon the change of the interaction constant c. To uncover it, in Fig. 1(b) we study the ground-state chemical potential μ as the function of interaction constant c. In view of Fig. 1(b), one sees that the curve of $F(\rho) \sim |\Phi|^2$ matches well the one using full $F(\rho)$ when $c < 1$. Therefore the present Bose gas can be taken to be in the weakly interacting limit when $c < 1$. It is noted that the point $c = 0.0009$, marked by "+" sign, is what used in Ref. [6] to discuss the nonlinear bands. The difference between the two curves increases with the increase of c. On the other side, the curve using full $F(\rho)$ matches well the one of $F(\rho) \sim |\Phi|^4$ when $c > 4$. Therefore the present Bose gas can be considered to be in the strong TG gas limit when $c > 4$.

IV. GAP SOLITONS AND BLOCH WAVES

When the nonlinear interaction term $F(\rho)$ is set to zero, Eq. (5) turns into the well-known linear Mathieu equation [2]. Its eigenfunctions are linear Bloch waves (LBWs) and eigenvalues form the linear Bloch band (LBB). Physical solutions are forbidden in the band gaps between neighboring bands. However, when the nonlinear interaction exists [$F(\rho) \neq 0$], two kinds of solutions can exist in the LBB gaps. One is the gap soliton and another is the NLBW. Both of them can share the same chemical potential in the LBB gaps. It has been illustrated in Ref. [6] that for the weak limit, $F(\rho) \sim |\Phi|^2$, the first nonlinear Bloch band (NLBB) can be lifted into the second, third, and higher LBB gaps with the increase of the scattering length g. Similarly the second NLBB can also be lifted into the third and higher LBB gaps. Consequently in the weak limit, NLBB in the nth LBB gap should include n-1 branches which are lifted from the lower levels. There is only one branch of NLBB that can develop in the lowest LBB gap [6]. The present issue is to check whether the above results remain correct in a more realistic model such that the nonlinear interaction term is described by the full $F(\rho)$. Our following numerical results will provide strong evidences that the above results remain valid for the whole span of the interaction regimes.

It is worth noting that as shown in Ref. [25], mean-field theory of Eq. (1) may not correctly describe the physics of a 1D impenetrable Tonks gas. This means that in the Tonks limit, a solitonic solution may not really exist. While this poses a limit on the solitonic solutions that we have obtained, it is still interesting to experimentally verify our theoretical predictions.

A. Interaction-dependent gap solitons and nonlinear Bloch bands

We first set $F(\rho) = 0$ to solve the linear Schrödinger equation (5) exactly by the finite-element method. The periodic potential strength v-dependent lowest four bands and band gaps are shown in Fig. 2(a). As shown, with the increase of v, the continuum energy spectrum turns into energy bands with gaps. When v is large enough, some (lower) bands reduce to highly-degenerate thin levels. We next retain $F(\rho)$ to solve the nonlinear Schrödinger equation (5) numerically. In particular, we are interested in the solutions of FGSs (or NLBWs) with the energy μ falling into the LBB gap regions. The numerical solutions are obtained by differentiating Eq. (5) on a finite difference grid to obtain a coupled algebraic equations and solve it with the Newton-relaxation method [5].

Figure 2(b) shows particle number N of gap solitons as the function of μ for four different interaction constant c's. As shown, for example, when $c = 3$ close to the strong limit (solid lines), the first NLBB develops from the first LBB and is lifted with the increase of N. The so-called NLBB lifting is simply due to the fact that the larger N is, the larger the nonlinearity and hence the corresponding μ are. The first NLBB enters the second LBB gap at $N \simeq 2.38$ and when $N \simeq 4.92$ it further enters the third LBB gap. For the second NLBB, it develops from the second LBB at $N \simeq 0.14$ and is lifted in a similar manner with the increase of N. It enters the third LBB gap when it crosses the critical value of $N \simeq 3.06$. It turns out that the third NLBB only devel-

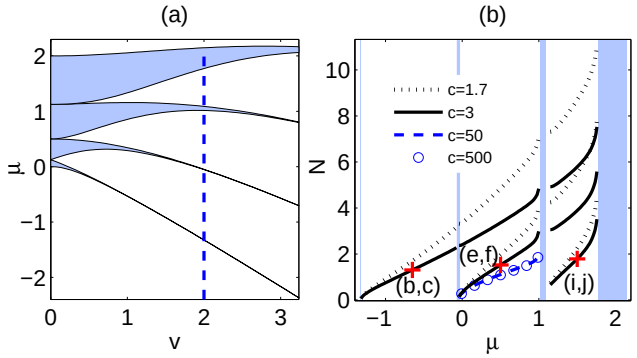

FIG. 2. (Color online) Panel (a): Energies μ of the lowest four linear Bloch bands and band gaps versus the strength of the periodic potential v. μ and v are in units of $8E_r$ with E_r the recoil energy (see text). The dashed line denotes $v = 2$ used in the calculations of panel (b). Panel (b): Particle number N of FGSs as the function of chemical potential μ for different interaction constant $c = 1.7$, 3, 50, and 500, respectively. The points marked by red "+"sign are those studied in Fig. 4.

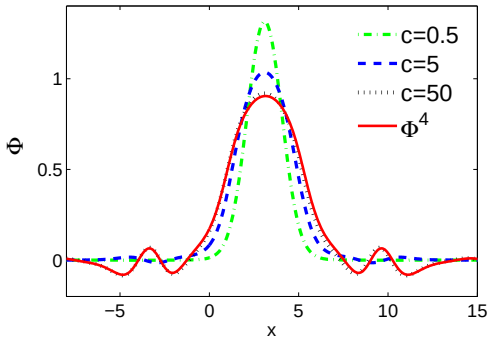

FIG. 3. (Color online) Amplitudes of the first-family FGS as the function of the interaction constant c. For all curves, particle number is fixed at $N = 3$ and periodic potential strength is $v = 2$. For comparison, the case of the strong interaction limit, $F(\rho) \sim |\Phi|^4$, is also shown.

ops at $N \gtrsim 0.66$, slightly above the third LBB.

For relatively weaker interaction case, $c = 1.7$ (dotted lines), the NLBB is seen to correspond to larger N for the same μ, as compared to those of the $c = 3$ case. This is because for the smaller interaction constant c, one needs a larger N to achieve the same nonlinear effect. We have also calculated the extremely strong interaction cases (for $c = 50$ and 500) for energies within the second LBB gap. The lines of the two cases are seen to coincide and indicate that the current Bose system is reduced to the TG gas when the interaction constant c is large enough.

B. Interaction-dependent amplitude of gap solitons

The soliton wave occurs only in the nonlinear system and has no classical correspondence. One may guess that the amplitude of soliton wave increases with the increase of the nonlinearity. However, the truth is in the opposite direction. As shown in Fig. 3, numerical results of the first-family FGS waves show that their amplitudes actually decrease as c increases. For all curves in Fig. 3, particle number is fixed at $N = 3$ and periodic potential strength is $v = 2$. For comparison, we have also shown the case for the strong interaction limit $[F(\rho) \sim |\Phi|^4]$.

In fact, FGSs originate from the nonlinearity and periodicity of the system. On one hand, FGSs can be taken roughly as the discrete eigenstates of the system in a single potential well. On the other hand, FGSs are eigenstates of the Schrödinger equation (5) if $[V(x) + F(\rho)]$ is taken approximately as the effective field of a single well. When the interaction constant c is increased and for the particle number N fixed, the confinement due to the effective single well will become weaker. This means that the wave function will become more dispersed and correspondingly the amplitude of the FGSs will become smaller.

C. Composition relation at strong interactions

As shown previously, NLBB can be viewed as the lifted LBB by increasing the nonlinear interaction. While LBB can be viewed as the evolution from the discrete energy levels of an individual well. Therefore it is not difficult to see that NLBW belonging to the nth NLBB should have n-1 nodes (in the sense of the nth bound state) in an individual well of the periodic potential. It has been pointed out and proven numerically for the weak interaction limit $[F(\rho) \sim |\Phi|^2]$ that FGSs which can only exist in a nonlinear system are the building blocks of the NLBWs [6]. Thus it is expected that FGS should behave like the bound states in an individual well of the periodic potential. The current issue is to verify whether the above conclusion remains correct when the nonlinear term is replaced by the full $F(\rho)$.

In Fig. 4, we solve and plot both NLBW (blue dashed line) and FGS (red solid line) for the relatively strong interaction ($c = 3$) case. It should be emphasized that the conclusion drawn here remains valid for much more stronger interaction cases. We consider both NLBWs and FGSs in the first, second, and third LBB gap respectively and for the representative we take the k points at both the BZ center ($k = 0$) and boundary ($k = 0.5$). In view of Fig. 4(b)&(c) with $\mu = -0.65$ and $N = 1.30$, an almost perfect match is found between the NLBW and the FGS within one unit cell in the first LBB gap. The good match occurs regardless of at the center or at the edge of the BZ. It thus gives a strong evidence that FGSs can be considered as the building blocks of the NLBWs. It is important to note that the waves shown in Fig. 4(b)&(c) are belonging to the first-family FGS and hence of no node. In Fig. 4(e)&(f), a good match is also found between the NLBW and the FGS within one unit cell in the second LBB gap. These waves with $\mu = 0.5$ and

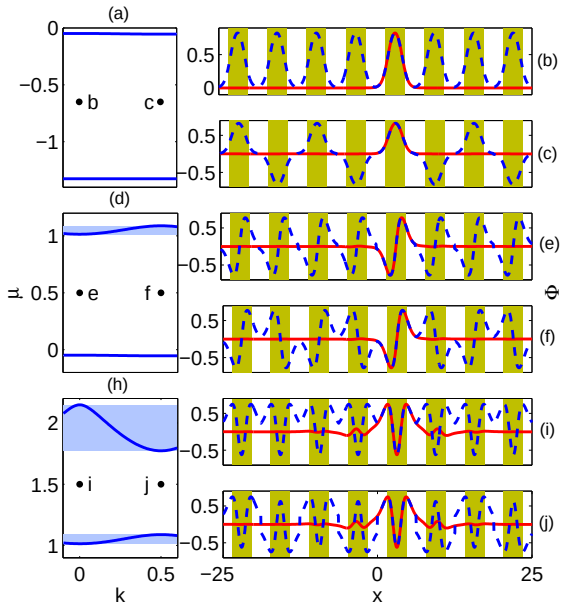

FIG. 4. (Color online) Left column: panel (a),(d), and (h) show the first, second, and third LBBs and band gaps. Thick black dots denote the (k, μ) points studied in the right column. Right column: panel (b) and (c) are the FGS (red solid line) and NLBW (blue dashed line) in the first LBB gap with $N = 1.30$ and $(k, \mu) = (0, -0.65)$ (at BZ center) and $(0.5, -0.65)$ (at BZ edge) respectively. Panel (e) and (f) are the FGS and NLBW in the second LBB gap with $N = 1.52$ and $(k, \mu) = (0, 0.5)$ and $(0.5, 0.5)$ respectively; panel (i) and (j) are the FGS and NLBW in the third LBB gap with $N = 1.79$ and $(k, \mu) = (0, 1.5)$ and $(0.5, 1.5)$ respectively. For all panels, the interaction constant is $c = 3$ and the periodic potential strength is $v = 2$. The (N, μ) points under study are also marked in Fig. 2(b).

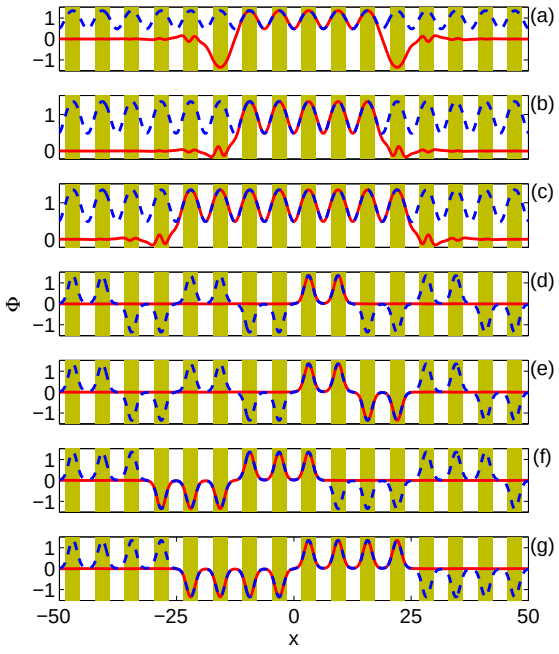

FIG. 5. (Color online) Panel (a)–(c): Illustration of the high-order gap solitons (red solid line) and NLBWs (blue dashed line) for $c = 3$ and $\mu = 1.63$. (a) The upper power branch of five-peak gap solitons; (b) The lower power branch of five-peak gap solitons; (c) The lower power branch of eight-peak gap solitons. Panel (d)–(g): Illustration of the high-order gap solitons (red solid line) and multiple periodic waves (blue dashed line) for $c = 0.3$ and $\mu = -1.07$. (d) Two-peak solitons with $N = 6$; (e) Solitons of two peaks up and two peaks down with $N = 12$; (f) Solutions of three peaks up and three peaks down with $N = 18$; (g) Solitons of four peaks up and four peaks down with $N = 24$. The periodic potential strength is $v = 2$ for all panels.

$N = 1.52$ are belonging to the second-family FGS and hence of one node. There is a key difference between the NLBWs in Fig. 4(b) and (c) such that the waves are oscillating in-phase ($k = 0$) between the neighboring wells in case (b), while it is out-of-phase ($k = 0.5$) in case (c). Similar consequence is also seen between Fig. 4(e) and (f) and also between Fig. 4(i) and (j).

As a test, we actually try to build the possible NLBWs using the first obtained third-family FGS in the third LBB gap [see Fig. 4(i) and (j)]. These third-family FGSs with $\mu = 1.5$ and $N = 1.79$ are obtained by the Newton-relaxation method with proper initial condition. To capture the out-of-phase motion of the NLBWs at the BZ edge [case (j)], we have added an alternative negative sign to the building block. In view of Fig. 4(i) and (j), the match between the NLBW and FGS is good except FGS exhibits a short tail across the cell boundary. Nevertheless, one can still conclude that the composition relation between NLBWs and FGSs is valid to a good approximation.

D. Generalized composition relation

In addition to the FGSs and NLBWs studied previously, there are two types of waves which are also common in a nonlinear system. One is called the high-order gap solitons which are gap soliton waves of multiple peaks over multiple unit cells [26]. As we will show later, high-order gap solitons can be viewed as the truncated NLBW and hence NLBWs can be built from them. Another is called the multiple periodic waves which are defined as $\Phi(x) = \exp(ikx)\psi_k(x)$ with $\psi_k(x) = \psi_k(x + 2n\pi)$ and n being a positive integer [27]. In the weakly interacting limit, it has been shown that composition relation between the FGSs and the NLBWs can be generalized to construct multiple periodic waves from the high-order gap solitons [7]. The present issue is again to see whether the generalized composition relation remains valid in the strong interaction limit.

We have first solved the time-dependent nonlinear Schrödinger equation (1) numerically using the imaginary-time method to obtain NLBW function $\Phi(x)$ and chemical potential μ with a given interaction con-

stant c. The Newton-relaxation method is then used to solve the time-independent nonlinear Schrödinger equation (5) with the pre-obtained μ and the proper initial condition. Fig. 5(a)–(c) show the five- and eight-peak high-order gap solitons with the interaction constant $c = 3$. An almost perfect match is found between the high-order gap solitons and the NLBWs. Thus high-order gap solitons can also be viewed as the truncated NLBWs for the strong interactions.

Fig. 5(d)-(g) show the composition relation between the high-order gap solitons and multiple periodic waves. Here $c = 0.3$ is used. Shown in Fig. 5(d) is the building block of two-peak high-order gap solitons which generates the two-peak up and two-peak down multiple periodic wave. Fig. 5(e) shows the same two-peak up and two-peak down multiple periodic wave that can also be built by the two-peak up and two-peak down high-order gap solitons. We further show the three-peak up and three-peak down and four-peak up and four-peak down multiple periodic waves in Fig. 5(f) and (g) built by the three-peak up and three-peak down and four-peak up and four-peak down high-order gap solitons respectively. The matches between the higher-order gap solitons and multiple periodic waves are all seen to be good. This stands that for the whole range of the interactions, FGSs are the most basic building blocks which can be used to build high-order solitons and multiple periodic waves.

V. STABILITY OF THE SOLITON WAVES

Stability of the FGS is another important issue when the interaction of the system is changed from the weak to the strong limit. We shall study the linear stability of FGS solution following the standard procedure. Since the unstable solution is sensitive to a small perturbation, one can add a small perturbation $\Delta\Phi(x,t)$ to a known solution $\Phi(x)$

$$\Psi(x,t) = [\Phi(x) + \Delta\Phi(x,t)]\exp(-i\mu t),$$

where $\Delta\Phi(x,t) = u(x)\exp(i\alpha t) + w^*(x)\exp(-i\alpha^* t)$. Inserting the perturbation into Eq. (1) and dropping the higher-order terms in (u, v), one then obtains the linear eigenequation

$$\begin{pmatrix} \mathcal{L} & -\frac{\partial F(\rho)}{\partial \rho}\Phi^2 \\ \frac{\partial F(\rho)}{\partial \rho}\Phi^{*2} & -\mathcal{L} \end{pmatrix} \begin{pmatrix} u \\ w \end{pmatrix} = \alpha \begin{pmatrix} u \\ w \end{pmatrix}, \quad (6)$$

where $\mathcal{L} \equiv \frac{1}{2}\frac{d^2}{dx^2} - V(x) - F(\rho) - \frac{\partial F(\rho)}{\partial \rho}|\Phi(x)|^2 + \mu$. Linear stability of a soliton is determined by the energy spectrum of the linear eigenequation (6). Among all eigenvalues α obtained, if there exists one of a finite imaginary part, the solution of $\Phi(x)$ would be unstable. Otherwise, the solution of $\Phi(x)$ is stable.

The stability of FGSs is investigated in Fig. 6. For the weak interaction case ($c = 1$), the linear stability analysis indicates that the first family FGSs which develop

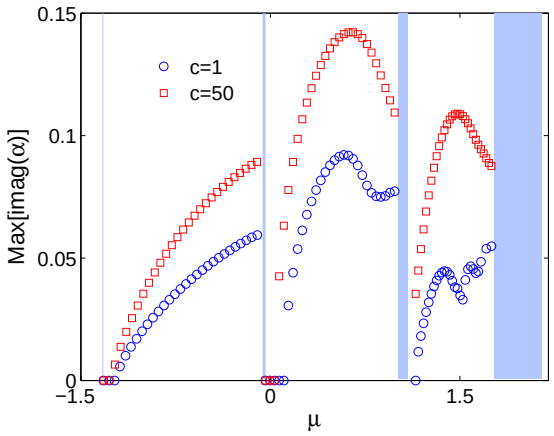

FIG. 6. (Color online) Studies of the stability of the FGSs in the first, second, and third LBB gap for weak ($c = 1$) and strong ($c = 50$) interaction limits. The periodic potential strength used is $v = 2$.

from the first LBB are stable when their chemical potentials μ are near the bottom of the first LBB gap. They will become unstable when μ becomes higher within the first band gap (with the increase of N), and enters into the second and third band gaps (not shown in Fig. 6). Similarly for the second family FGSs which develop from the second LBB, they are also stable when the chemical potentials are near the bottom of the second band gap. While for the third family FGSs, they are stable only when μ is extremely close to the bottom of the third band gap. In contract, for the strong interaction case ($c = 50$), studies of linear stability indicate that stable FGSs of the first and second families exist only in a much narrower regime with μ near the bottom of the band gaps; while it seems that the third-family FGSs can no longer be stable. Bearing the above results, it is argued that stable FGSs can be easily formed in a weakly interacting system with chemical potential near the bottom of the lower-level band gaps.

For completeness, we have also investigated the stability of two kinds of five-peak gap solitons. One is the upper power branch shown in Fig. 5(a) and another is the lower power one shown in Fig. 5(b) [26]. The linear stability analysis was carried out in the first LBB gap for three chemical potentials, $\mu = -1.3$, -1.22, and -1.2 respectively and the results are shown in Fig. 7. For the case of $\mu = -1.3$, five-peak gap solitons are stable for both upper [see Fig. 7(f)] and lower power branches [see Fig. 7(e)]. This is consistent with the case of FGSs which are stable with μ near the bottom of the LBB gap. For the case of $\mu = -1.22$ near the middle of the first band gap, the lower power branch of five-peak gap solitons are still stable [see Fig. 7(c)], while the upper power branch of five-peak gap solitons become unstable [see Fig. 7(d)]. This is consistent with the one analysis studied in Ref. [26]. When μ is increased to be -1.2,

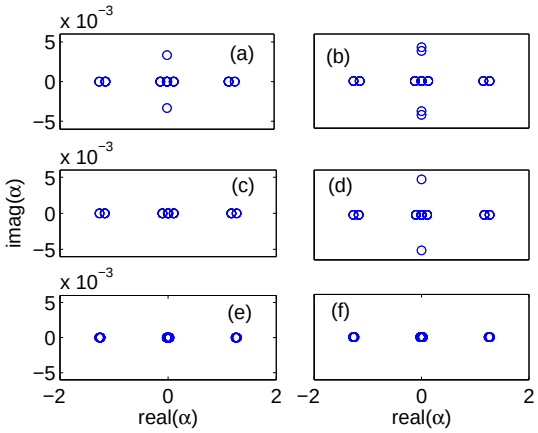

FIG. 7. (Color online) Linear-stability studies of the five-peak gap solitons in the first LBB gap. Panel (a), (c), and (e) correspond to the lower power ones shown in Fig. 5(b), while panel (b), (d), and (f) correspond to the upper power ones shown in Fig. 5(a). Chemical potential $\mu = -1.3$ for (e) and (f), -1.22 for (c) and (d), and -1.2 for (a) and (b). Interaction constant $c = 1$ and periodic potential strength is $v = 2$.

five-peak gap solitons are unstable for both the lower [see Fig. 7(a)] and upper power branches [see Fig. 7(b)]. Therefore, the stable multi-peak solitons can also be easily formed with μ near the bottom of the lower band gaps.

The stability of the multi-peak solitons upon the change of the periodic potential strength (v) is also studied. It is found that all the unstable multi-peak solitons studied in Fig. 7 will eventually become stable when v is increased from the present value 2 to 10. The reasons behind it are easily understood. When v is increased, interaction is reduced relatively. Consequently chemical potential will approach relatively closer to the bottom of the LLB gap and gap solitons will become relatively more stable.

VI. SUMMARY

In summary, we have investigated the composition relation between the fundamental gap solitons (FGSs) and nonlinear Bloch waves (NLBWs) of interacting bosons in one-dimensional optical lattices. The main focus is to consider the interaction from the weak to the strong limits. Our numerical results verify that the composition relation remains correct in the whole span of the interaction strength. FGSs are thus the fundamental building blocks to build all other stationary solutions, including NLBWs, high-order solitons, and multiple periodic waves, in one-dimensional nonlinear periodic systems. By the linear stability analysis, it is found that the stable FGSs exist near the bottom of the linear band gap. By increasing the interaction strength, the stable gap solitons will become unstable. However, one can restore the stability of the unstable FGSs by increasing the strength of the periodic potential. It is argued that the stable gap solitons can be easily formed in a weakly interacting system with the chemical potential near the bottom of the lower-level band gaps.

ACKNOWLEDGMENTS

We thank Yong-Ping Zhang, Biao Wu, and Shu Chen for useful discussions. This work is supported by National Science Council of Taiwan (Grant No. 99-2112-M-003-006), Hebei Provincial Natural Science Foundation of China (Grant No. A2010001116), and the National Natural Science Foundation of China (Grant No. 10974169). We also acknowledge the support from the National Center for Theoretical Sciences, Taiwan.

[1] O. Morsch and M. Oberthaler, Rev. Mod. Phys. **78**, 179 (2006).
[2] N. W. Aschcoft and N. D. Mermin, *Solid State Physics* (1976).
[3] Y. Kivshar and G. Agrawal, *From Fibers to Photonic Crystals* (2003) p. 540.
[4] P. J. Y. Louis, E. A. Ostrovskaya, C. M. Savage, and Y. S. Kivshar, Phys. Rev. A **67**, 013602 (2003).
[5] T. Mayteevarunyoo and B. A. Malomed, Phys. Rev. A **74**, 033616 (2006).
[6] Y. Zhang and B. Wu, Phys. Rev. Lett. **102**, 093905 (2009).
[7] Y. Zhang, Z. Liang, and B. Wu, Phys. Rev. A **80**, 063815 (2009).
[8] E. H. Lieb and W. Liniger, Phys. Rev. **130**, 1605 (1963).
[9] D. S. Petrov, G. V. Shlyapnikov, and J. T. M. Walraven, Phys. Rev. Lett. **85**, 3745 (2000).
[10] V. Dunjko, V. Lorent, and M. Olshanii, Phys. Rev. Lett. **86**, 5413 (2001).
[11] S. Chen and R. Egger, Phys. Rev. A **68**, 063605 (2003).
[12] O. E. Alon and L. S. Cederbaum, Phys. Rev. Lett. **95**, 140402 (2005).
[13] Y. Hao, Y. Zhang, J. Q. Liang, and S. Chen, Phys. Rev. A **73**, 063617 (2006).
[14] M. D. Girardeau and A. Minguzzi, Phys. Rev. Lett. **99**, 230402 (2007).
[15] B. Sutherland, Phys. Rev. Lett. **20**, 98 (1968).
[16] Y.-Q. Li, S.-J. Gu, Z.-J. Ying, and U. Eckern, EPL (Europhysics Letters) **61**, 368 (2003).
[17] M. Zhong-Qi and C. N. Yang, Chin. Phys. Lett. **26**, 120506 (2009).
[18] M. Zhong-Qi and C. N. Yang, Chin. Phys. Lett. **27**, 020506 (2010).
[19] Y. Hao and S. Chen, Phys. Rev. A **80**, 043608 (2009).

[20] C. Johnson, *Numerical Solution of Partial Differential Equations by the Finite Element Method,* (Studentlitteratur, Lund, Sweden, 1987).
[21] M. D. Girardeau, Phys. Rev. **139**, B500 (1965).
[22] P. Vignolo, A. Minguzzi, and M. Tosi, Int. J. Mod. Phys. B **16**, 2161 (2002).
[23] F. Dalfovo, S. Giorgini, L. P. Pitaevskii, and S. Stringari, Rev. Mod. Phys. **71**, 463 (1999).
[24] E. B. Kolomeisky, T. J. Newman, J. P. Straley, and X. Qi, Phys. Rev. Lett. **85**, 1146 (2000).
[25] M. D. Girardeau and E. M. Wright, Phys. Rev. Lett. **84**, 5239 (2000).
[26] J. Wang, J. Yang, T. J. Alexander, and Y. S. Kivshar, Phys. Rev. A **79**, 043610 (2009).
[27] M. Machholm, A. Nicolin, C. J. Pethick, and H. Smith, Phys. Rev. A **69**, 043604 (2004).